의학박사 학위 논문

거세 저항성 전립선암에서 WNT 신호 전달 체계와 소포체 스트레스 조절에 대한 연구

Regulation of WNT signaling and endoplasmic reticulum stress in castration-resistant prostate cancer

울 산 대 학 교 대 학 원

의 학 과

박 사 현

거세 저항성 전립선암에서 WNT 신호 전달 체계와 소포체 스트레스 조절에 대한 연구

지 도 교 수　　안 한 종

이 논문을 의학박사 학위 논문으로 제출함

2021년 12월

울 산 대 학 교 대 학 원

의　　학　　과

박 사 현

박사현의 의학박사 학위 논문을 인준함

심사위원	홍 준 혁	인
심사위원	안 한 종	인
심사위원	송 채 린	인
심사위원	유 달 산	인
심사위원	권 오 성	인

울 산 대 학 교 대 학 원

2022년 2월

ABSTRACT

Several treatments improve survival associated with castration-resistant prostate cancer (CRPC). However, median CRPC survival is <2 years, and treatment is associated with acquired resistance. Therefore, new therapeutic targets and effective therapies for CRPC are needed. Growing evidence suggests that WNT/β-catenin signaling and endoplasmic reticulum (ER) stress play oncogenic roles. We explored the anti-CRPC activity of CWP232291, a small-molecule β-catenin inhibitor and ER stress inducer.

We evaluated the effects of CWP232291 on human prostate cancer cell lines and primary cells from patients. Apoptotic cell death, WNT/β-catenin signaling, and ER stress were analyzed using Western blotting, reverse transcription and quantitative polymerase chain reaction, immunofluorescence staining, confocal microscopy, flow cytometry, cytotoxicity assaying, dual-luciferase reporter assaying, annexin V and propidium iodide assaying, and chromatin immunoprecipitation assaying. Antitumor

activity was evaluated in 22Rv1 xenograft mouse models.

CWP232291 downregulated β-catenin activity, transcription, androgen receptors, and its splice variants in prostate cancer cells. Additionally, CWP232291 triggered ER stress, upregulating proapoptotic C/EBP-homologous protein and activating a caspase-3-dependent apoptotic cascade. CWP232291 suppressed the growth of CRPC cells and primary prostate cancer cells from patients and had in vivo antitumor activity in the 22Rv1 xenograft mouse model.

In conclusion, CWP232291 suppressed CRPC cell growth in vitro, ex vivo, and in vivo, demonstrating a potential CRPC treatment strategy involving WNT/β-catenin and ER stress regulation.

차 례

영문요약 · i

그림 차례 · iv

약어 목록 · vi

본문 · 1

참고문헌 목록 · 62

국문요약 · 70

그림 차례

Figure 1. CWP291 downregulates β-catenin and survivin levels in prostate cancer cells.22

Figure 2. Prostate cancer cells were treated with WNT3A and CWP291 for 24h and stained with β-catenin (green) or DAPI (blue). Images were obtained from a fluorescence microscope. ……24

Figure 3. CWP291 downregulates the ARs and splice variants. ……28

Figure 4. Prostate cancer cells were treated with 0–10 μM CWP291 for 72 h. The LDH cell cytotoxicity was evaluated with the Cytotoxicity Detection Kit. ……30

Figure 5. Androgen response elements reporter assay in LNCaP and 22Rv1 cells treated with or without DHT and CWP291 at the IC50.……31

Figure 6. 22Rv1 cells were androgen deprived for 48 h and treated with vehicle or DHT with or without CWP291 for 24 h. ……32

Figure 7. CWP291 suppresses the growth of prostate cancer cells and primary cells derived from patients. ……34

Figure 8. CWP291 triggers endoplasmic reticulum stress and the unfolded protein response in prostate cancer cells. ……38

Figure 9. CWP291 mediates cell cycle arrest and apoptosis in prostate cancer cells.……41

Figure 10. CWP291 suppresses the growth of prostate cancer xenografts.……44

Figure 11. 22Rv1 and 22Rv1-AbiR cells were exposed to 0–100 μM abiraterone acetate and 0–10 μM docetaxel for 72 h. Cell viability was analyzed with CellTiter Glo®.……47

Figure 12. 22Rv1 and 22Rv1-AbiR cells were exposed to 0–10 μM CWP291 for 72 h. Cell

viability was analyzed with CellTiter Glo®. ····· 50

Figure 13. CWP291 regulates WNT, AR, and ER stress signaling in AA-resistant prostate cancer cells. ····· 51

약어 목록

ADT: androgen deprivation therapy; AR: androgen receptor; ATF6: activating transcription factor 6; CHOP: C/EBP-homologous protein; CRPC: castration-resistant prostate cancer; DAPI: 4′,6-diamidino-2-phenylindole; DHT: dihydrotestosterone; FBS: fetal bovine serum; IRE1: inositol-requiring kinase 1; LDH: lactate dehydrogenase; LEF: lymphoid enhancer-binding factor; PARP: [poly (ADP-ribose) polymerase; PERK: protein kinase RNA-like ER kinase; RT-PCR: real-time polymerase chain reaction; TCF: transcription factor; UPR: unfolded protein response; ZVAD-FMK: z-valine-alanine-aspartate-fluoromethylketone.

Background

Prostate cancer is the second most commonly diagnosed cancer and the fifth leading cause of cancer death among males worldwide (1). Men with prostate cancer are generally considered to have favorable survival outcomes (2). However, advanced prostate cancer accounts for more than 15% of all diagnosed prostate cancers (3), which is more challenging to treat and may be incurable if metastatic (4).

Although androgen deprivation therapy (ADT) is usually effective for advanced prostate cancer initially (5, 6), resistance to ADT eventually develops in nearly all metastatic prostate cancer patients, leading to a status called castration-resistant prostate cancer (CRPC). In men with CRPC, the median survival is less than 2 years, and most patients die from metastatic progression (7). CRPC treatment remains a major challenge despite the availability of several active treatment options, including taxane-based chemotherapy and androgen receptor (AR) signaling inhibitors (8).

Aberrations in AR-related mechanisms, including increased androgen production,

mutation or amplification of receptors, alterations of co-activators, and splice variants, are among the key pathways in the development of castration resistance (9). Despite the survival benefits associated with AR-targeted treatments, such as abiraterone acetate (AA) (5) and enzalutamide (6), acquired resistance to AR signaling inhibitors eventually develops (10). Therefore, new therapeutic targets and effective therapies for CRPC are always needed. Moreover, it is important to understand underlying drug resistance mechanisms and identify new strategies to overcome drug resistance in patients with CRPC.

WNT signaling pathways are highly evolutionarily conserved pathways involved in embryonic development, as well as cell division and migration in multiple organ systems (11). WNT signaling proceeds through β-catenin-independent noncanonical pathways or β-catenin-dependent canonical pathways. In the absence of WNT signaling, β-catenin is captured and degraded by the glycogen synthase kinase 3β (GSK3β) and destruction complex (12). When the pathway is stimulated by the

binding of WNT to its receptors, β-catenin dissociates from the disrupted destruction complex, thereby inducing subsequent translocation to the nucleus (13).

Various human diseases, including cancer, are associated with WNT pathway malfunction (14). Accumulating evidence suggests that WNT pathway alteration plays a role in prostate cancer. Whole-exome sequencing of samples from heavily treated CRPC have been shown to have significantly mutated WNT signaling pathway–associated genes (15). The occurrence of crosstalk between AR and β-catenin in advanced prostate cancer is well known (16-22). In CRPC, nuclear interactions between AR and β-catenin are upregulated relative to castration-sensitive prostate cancer. Additionally, WNT pathways act as key modulators in PI3K/mTOR and MAPK pathways, which are highly associated with advanced prostate cancer (23). Therefore, WNT pathway signaling is considered a potentially promising target in the treatment of advanced prostate cancer, although treatment approaches using WNT signaling regulators remain largely uncharacterized.

The endoplasmic reticulum (ER) is a central organelle that plays important roles in cellular homeostasis and signaling (24). The ER serves many important functions, such as protein folding and synthesis. Correct folding of proteins is made possible by several ER chaperone proteins, including protein disulfide isomerase, calnexin, and BiP/Grp78. Many different conditions cause a disequilibrium between ER load and capacity, which is called ER stress. ER stress emerges as a potential cause of damage in hypoxia, ischemia, insulin resistance, and other disorders (25). ER stress in cancer cells, induced by internal or external factors, activates the unfolded protein response (UPR) (26). The pro-survival function of the UPR can induce mitochondrial apoptosis according to the severity and duration of ER stress (27). Several studies have demonstrated that targeting ER stress and the UPR pathway have antitumor activity in cancer cells (28-32), suggesting that regulating ER stress pathways may provide novel approaches for cancer treatment.

This study investigated the roles and regulation of WNT signaling and ER stress in

CRPC, using the novel small molecule CWP232291 (CWP291). The effect of WNT inhibition on AR signaling and antitumor activity in prostate cancer was evaluated in vitro, ex vivo, and in vivo. The majority of the content of this dissertation is based on previously published work that has been peer-reviewed in its majority (33).

Materials and methods

Reagents and antibodies

The compound z-valine-alanine-aspartate-fluoromethylketone (ZVAD-FMK) was purchased from R&D Systems (Minneapolis, MN, USA). The following primary antibodies were used:

β-catenin (Merck Millipore, Burlington, MA, USA), AR, AKR1C3, survivin, bcl-2, GAPDH, β-actin (Santa Cruz Biotechnology, Dallas, TX, USA), AR-V7 (Precision Antibody, Columbia, MD, USA), phospho-eIF2a serine 51 [peIF2a (serine-51)], eIF2a, inositol-requiring kinase 1 (IRE1), poly ADP-ribose polymerase (PARP), cleaved caspase-3, C/EBP-homologous protein (CHOP) (Cell Signaling Technology, Danvers, MA, USA). CWP291 was obtained from JW Pharmaceutical Corporation (Seoul, Korea).

Cell lines and cell culture

The human prostate cancer cell lines PC3, DU145, LNCaP, VCaP, and 22Rv1 were purchased from the American Type Culture Collection (Manassas, VA, USA) and retained in RPMI 1640 (Invitrogen, Waltham, MA, USA) with 5–10% heat-inactivated fetal bovine serum (FBS), 100 μg/mL streptomycin, and 100 units/mL penicillin in a 5% CO_2 atm at 37 °C. After approval by the institutional review board of Asan Medical Center, four CRPC patient tissues were obtained by transurethral resection of the prostate. CRPC specimens were minced finely with scissors and digested by incubation in RPMI containing 1 mg/mL type I collagenase (Sigma Aldrich, St. Louis, MO, USA) for 1 h at 37 °C. Cells were washed with a medium containing 10% FBS to inactivate collagenase and then with phosphate-buffered saline (PBS) to remove the FBS. Next, cells were plated and retained in Human Prostate Epithelial Cell Growth Medium (Lonza, Portsmouth, NH, USA) in a 5% CO_2 atm at 37 °C. Only low-passage cells (< passage 8–15) were used in the experiments to ensure consistency and

authenticity. Mycoplasma testing was performed using a polymerase chain reaction (PCR)–based e-mycoplasma test kit (iNtRON Biotechnology, Seongnam, Korea). Abiraterone-resistant prostate cancer cell lines were generated from parental 22Rv1 cells by long-term culturing in the presence of increasing amounts of AA. 22Rv1 abiraterone-resistant cells were cultured in 10–50 μM AA over 2 months and maintained in 5 μM AA-containing medium.

Western blotting

Whole-cell lysates were prepared in lysis buffer [150 mmol/L NaCl, 1% Nonidet P-40, 50 mmol/L Tris–HCl (pH 7.4), 50 mmol/L NaF, 5 mmol/L EDTA, 0.1 mmol/L Na_3VO_4, and 0.1% SDS] containing protease inhibitor cocktail (Sigma Aldrich). The cell lysates were microcentrifuged at 13,000 × g for 10 min, and the supernatants were stored at −80 °C. Protein concentration was measured using the Bradford protein assay (Bio-Rad, Hercules, CA, USA). Proteins were separated by electrophoresis and transferred

to a polyvinylidene fluoride (PVDF) membrane. After blocking with 5% bovine serum albumin (BSA) for 1 h at room temperature, the membranes were incubated with primary antibody and then with secondary antibody conjugated with peroxidase. Protein bands were detected using the chemiluminescence detection system (Millipore Corp., Billerica, MA, USA).

RNA extraction, reverse transcription, and quantitative PCR

Total RNA was extracted from control or CWP291-treated cell lines using Trizol® (Invitrogen) according to the manufacturer's instructions. The DNase-treated RNA was reverse-transcribed using a cDNA synthesis kit (Toyobo, Osaka, Japan). Quantitative PCR was performed using the SYBR method (Toyobo). The PCR thermal cycling conditions were as follows: 95 °C for 20 s, followed by 40 cycles of 95 °C for 3 s, and 60 °C for 30 s. The melting curve stage proceeded at 95 °C for 15 s, melting from 60 °C for 1 min to 95 °C for 15 s with a ramp rate of 1%, and 60 °C for 15 s. Melting curve analysis was conducted to ensure the specificity of the PCR products. GAPDH was used for internal reference and loading control. PCR-based amplification was performed using the following primers: CHOP forward, 5′-AGAACCAGGAAACGGAAACAGA-3′, reverse, 5′-

TCTCCTTCATGCGCTGCTTT-3′; AR forward, 5′-CAGTGGATGGGCTGAAAAAT-3′, reverse 5′-AAGCGTCTTGAGCAGGATGT-3′; PSA forward, 5′-CATCAGGAACAAAAGCGTGA-3′, reverse, 5′-ATATCGTAGAGCGGGTGTGG-3′; UBE2C forward, 5′-AGTGGCTACCCTTACAATGCG-3′, reverse, 5′-TTACCCTGGGTGTCCACGTT-3′; UGT2B17 forward, 5′-ACCAGCCAAACCCTTGCCTAAG-3′, reverse, 5′-GGCTGATGCAATCATGTTGGCAC-3′; TMPSS2 forward, 5′-CAGGAGTGTACGGGAATGTGATGGT-3′, reverse, 5′-GATTAGCCGTCTGCCCTCATTTGT-3′; c-myc forward, 5′- GCTGCTTAGACGCTGGATTT-3′, reverse, 5′-GGCATTCGACTCATCTCAGC-3′; cyclin D1 forward, 5′-ATGTTCGTGGCCTCTAAGATGA-3′, reverse, 5′-CCAGTGGTTACCAGCAGCTC-3′; MMP-7 forward, 5′-TGAGCTACAGTGGGAACAGG-3′, reverse, 5′-ACCACCCCAAAGAAAATTCC-3′; Annexin-2 forward, 5′-ACGCTGGAGTGAAGAGGAAA-3′, reverse, 5′-AAGGCACTGAGACTCCCTCA-3′; Axin-2 forward, 5′-AGTGTGAGGTCCACGGAAAC-3′, reverse, 5′-TGGCTGGTGCAAAGACATAG-3′; and GAPDH forward, 5′-CAATGACCCCTTCATTGACC-3′, reverse, 5′-GACAAGCTTCCCGTTCTCAG-3′.

Immunofluorescence staining and confocal microscopy

Cells were fixed with 4% paraformaldehyde in PBS for 20 min and permeabilized with 0.1% Triton X-100 (Sigma Aldrich) in PBS for 30 min. Nonspecific binding sites were blocked with 5% BSA in PBS for 1 h, and then cells were incubated overnight at 4 °C with primary antibody against AR followed by secondary antibody conjugated with fluorescent dye (Molecular Probes, Eugene, OR, USA). The samples were mounted in Vectashield medium containing 4′,6-diamidino-2-phenylindole (DAPI) (Vector Laboratories, Burlingame, CA, USA). Confocal images were obtained using a confocal laser scanning microscopy system (Leica Geosystems, Heerbrugg, Switzerland).

Cell viability assay

Cell viability was evaluated using the CellTiter Glo® cell viability assay (Promega, Madison, WI, USA). Briefly, 3×10^3 cells were seeded per well in 96-well plates and

incubated overnight. After exposure to CWP291, cells were incubated with 20 µL of CellTiter Glo reagent for 10 min, after which luminescence intensity was evaluated on a MicroLumatPlus LB luminometer (EG&G Berthold, Bad Wildbad, Germany). All plates had blank wells containing cell-free medium to calculate background luminescence. Data represent the percentage of control without treatment [(treatment value − blank)/(vehicle value − blank)] expressed as the mean ± standard deviation (SD) of at least three repetitions. Results were analyzed using GraphPad Prism, version 6 (GraphPad Software Inc., San Diego, CA, USA). Half-maximal inhibitory concentration (IC_{50}) values were determined for each cell line as the concentration required to inhibit the control by 50%.

Cell cytotoxicity assay

The lactate dehydrogenase (LDH) cytotoxicity assay was conducted using the Cytotoxicity Detection Kit (Sigma Aldrich) according to the manufacturer's

instructions. Briefly, 3×10^3 cells were seeded per well into 96-well plates and incubated overnight. After treatment with CWP291, 50 μL of sample medium (from control and concentration-dependent treatments) were transferred to 96-well plates in triplicate. Reaction mixture (50 μL) was then added to each sample and incubated for 30 min in the dark at room temperature. The reaction was stopped by adding 50 μL of stop solution and mixing by gentle tapping. The absorbance was measured at 492 nm and 680 nm. The 680 nm absorbance value (background) was subtracted from the 492 nm absorbance value before calculation of percent cytotoxicity. The maximum LDH activity was determined after treating cells with lysis buffer as described in the manufacturer's instructions. Cytotoxicity (%) was calculated using the following formula:

cytotoxicity (%) = (CWP-treated LDH activity − low LDH activity)/(high LDH activity − low LDH activity) × 100

Transient transfection and dual-luciferase reporter assay

The TCF/LEF reporter construct is a mixture of an inducible β-catenin–responsive firefly luciferase reporter and constitutively expressing Renilla construct. The β-catenin–responsive luciferase construct encodes the firefly luciferase reporter gene under the control of a minimal (m)CMV promoter and tandem repeats of the TCF/LEF transcriptional response element. For transfection, cells were seeded at 3×10^5 cells/well (PC3 and DU145) and 6×10^5 cells/well (LNCaP and 22Rv1) in 6-well plates. After 18–24 h, cells were transfected with 1 μg of TCF/LEF reporter construct (Qiagen GmbH, Hilden, Germany) using 2 μL of Lipofectamine 2000™ (Invitrogen) in 50 μL of OptiMEM® reduced-serum medium, achieving a DNA/Lipofectamine 2000™ ratio of 1:2. After transfection, cells were treated with or without CWP291 and 100 ng/mL WNT3A (R&D Systems) for 24 h; control cells were untreated. Luciferase assays were performed using the Dual-Glo luciferase assay system (Promega). Each assay was conducted in triplicate, and the reporter activity was expressed as mean ± SD.

Androgen response element reporter assay

The androgen response element reporter assay was performed using the androgen receptor reporter kit (Qiagen, Toronto, ON, Canada). LNCaP and 22Rv1 cells were transfected with a mixture of an inducible androgen receptor–responsive firefly luciferase reporter and construct constitutively expressing Renilla luciferase (40:1 ratio). The AR-responsive luciferase construct encodes the firefly luciferase reporter gene under the control of a CMV promoter and tandem repeats of the AR transcriptional response element. Twenty-four hours after cells were transfected with the inducible androgen response element luciferase construct in the presence or absence of CWP291 (LNCaP; 100 nM, 22Rv1 60 nM) and dihydrotestosterone (DHT; 10 nM), the luciferase activities of the cells were measured with a Dual-Glo luciferase reporter assay kit (Promega).

Apoptosis assay

Cells were seeded in 6-well plates in RPMI 1640 medium containing 10% FBS for 18–24 h. The cells were then treated with CWP291 for 72 h, after which apoptosis and necrosis were assessed by flow cytometry using the annexin V-FITC apoptosis detection assay (BD Biosciences, Bedford, MA, USA) in accordance with the manufacturer's instructions. In this assay, cells positive for annexin V (bottom right quadrant) and those positive for both annexin V and propidium iodide (PI) (top right quadrant) represent the early and late apoptotic populations, respectively, whereas cells positive for PI only (top left quadrant) represent the necrotic population. The apoptosis cell population analysis was carried out using CellQuestPro software (BD Biosciences, Franklin Lakes, NJ, USA).

Chromatin immunoprecipitation assay

After 22Rv1 cells were androgen-deprived for 48 h, they were treated with vehicle or 10 nM DHT with or without 60 nM CWP291 for 24 h. Cells were fixed in 1% formaldehyde at room temperature, and the cross-linking reaction was stopped with 125 mM glycine. After cell lysis, chromatin was digested into 150–500 bp fragments using a sonicator (power, 3 W; sonication time, 20 s; number of repeats, 3), and protein-DNA complexes were immunocaptured by mixing magnetic bead-coated anti-β-catenin antibody (10 μg; Santa Cruz Biotechnology) with the fragmented chromatin on a rotator at 4 °C overnight. After washing and reversal of cross-links, the IP DNA and input DNAs were purified and amplified by PCR. Relative enrichment was calculated as a percentage of 1% input normalized to IgG. The forward (CAAAATTGAGCGCCTATGTG) and reverse (TTGCTCTAGGAACCCTCAGC) primers of the TCF-binding site on the AR promoter were used.

Tumor xenograft models

The experiment protocols were approved by the institutional animal care and use committee of Asan Medical Center. The 22Rv1 cells (5×10^6) were injected subcutaneously into the right dorsal flanks of 6-week-old male BALB/C nude mice (OrientBio, Seoul, Korea). When the tumors reached a mean volume of 70–100 mm^3, the mice were randomly categorized into two groups: control and treatment. Mice in the treatment group were treated with CWP291 in 3% dimethyl sulfoxide in PBS, and the control mice received an equal volume of the corresponding diluent alone. The 22Rv1-bearing mice received intravenous (tail vein) CWP291 (50 or 100 mg/kg) or vehicle alone once per week for 4 weeks (n = 6 per group). The tumor volume was measured three times a week and calculated using the following formula: $0.52 \times \text{length} \times (\text{width})^2$ (length: longest diameter across the tumor; width: corresponding perpendicular diameter).

Statistical analysis

Results are reported as means ± SD. Data were obtained from at least three independent experiments. Statistical analysis of the results was performed by one-way or two-way ANOVA with the Dunnett multiple comparisons test. *P* values <0.05 were considered statistically significant. Statistical differences between groups were evaluated using GraphPad Prism, version 6 (GraphPad Software Inc.).

Results

Suppression of WNT/β-catenin activity by CWP291

CWP291, a novel small molecule, inhibits β-catenin and triggers ER stress (34). Human prostate cancer cell lines, PC3 and DU145 (androgen-independent and AR-negative), LNCaP (androgen-dependent and AR-positive), and 22Rv1 (androgen-independent and AR-positive), were used.

First, we investigated whether CWP291, a WNT/β-catenin inhibitor and ER stress inducer, triggers apoptotic cell death in prostate cancer cells. In the canonical WNT pathway, LEF/TCF family members are the key mediators of β-catenin-dependent transcription (14, 35). To investigate the targeting transcriptional activity of WNT/β-catenin signaling, prostate cancer cells were transfected with a TCF/LEF luciferase reporter plasmid and treated with IC_{50} doses of CWP291 (PC3, 200 nM; DU145, 400 nM; LNCaP, 60 nM; 22Rv1, 70 nM) in the presence or absence of WNT3A (Fig. 1A).

After CWP291 treatment, significantly reduced luciferase expression was observed relative to the control. Western blot analysis revealed that CWP291 significantly inhibited the levels of β-catenin and the downstream protein survivin in prostate cancer cells in a dose-dependent manner (Fig. 1B). Additionally, a reduction (relative to the control) of nuclear staining of β-catenin after CWP291 treatment was observed by fluorescence microscopy. Without CWP291, β-catenin activity was observed diffusely across the cytoplasm, while WNT stimulation increased the nuclear expression and localization of β-catenin (Fig. 2). Nuclear staining for β-catenin was reduced after CWP291 treatment compared with the control (Fig. 1C).

Next, we tested whether WNT target gene expression would be influenced by CWP291 treatment. In LNCaP and 22Rv1 cells, the mRNA expression levels of c-myc, cyclin D1, MMP-7, and annexin-2 decreased after CWP291 exposure for 24 h compared with the control (Fig. 1D).

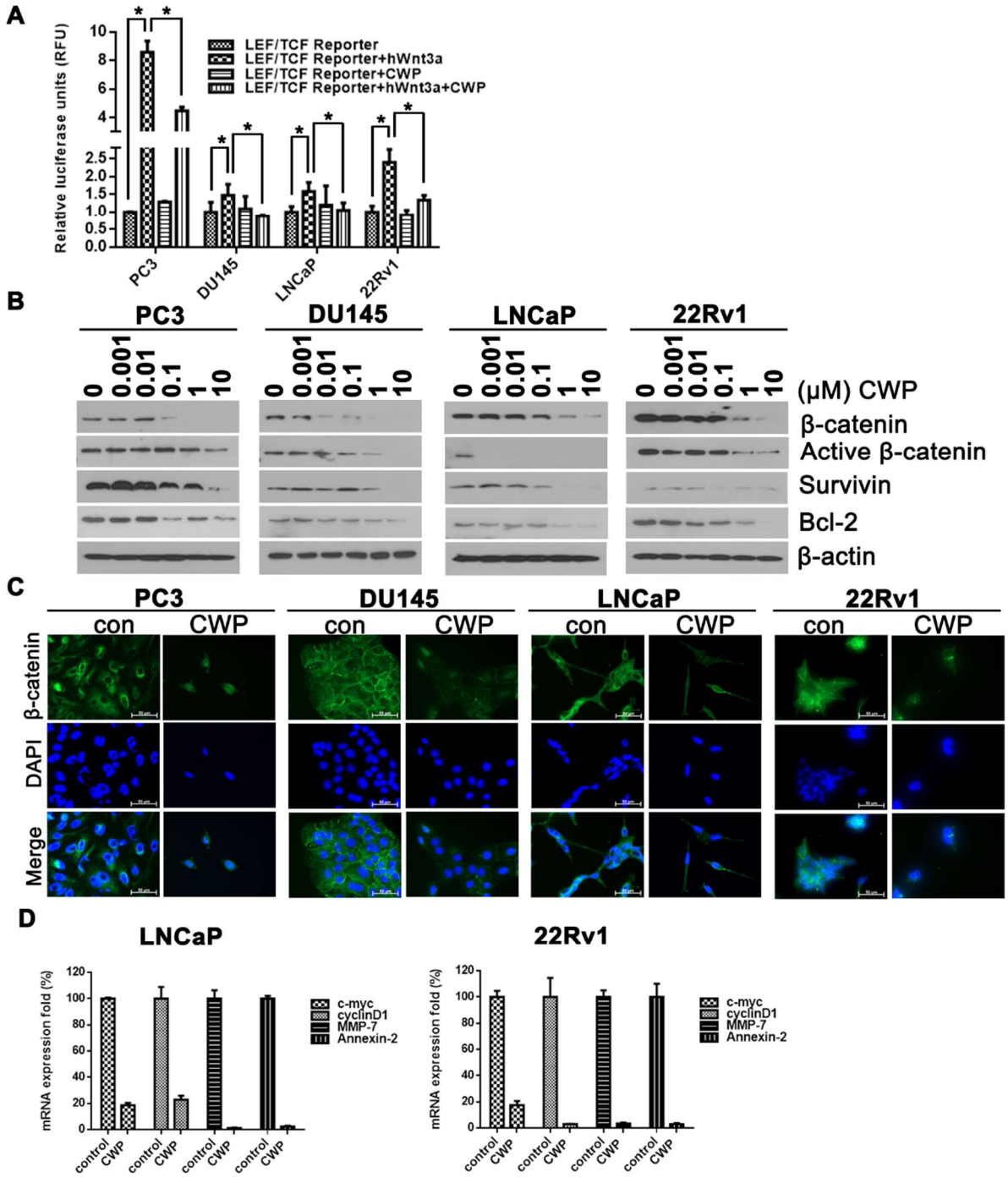

Figure 1. CWP291 downregulates β-catenin and survivin levels in prostate cancer cells.

(A) Luciferase reporter assay for WNT signaling after treatment with or without WNT3A (100 ng/mL) and IC_{50} doses of CWP291 in prostate cancer cells.

(B) Prostate cancer cells were treated with CWP291 for 24 h. Protein levels of β-catenin, survivin, and bcl-2 were evaluated by Western blotting.

(C) Prostate cancer cells were treated with CWP291 for 24 h and stained with β-catenin (green) or DAPI (blue). Images were obtained via fluorescence microscopy.

(D) LNCaP and 22Rv1 cells were treated with or without CWP291 for 24 h. mRNA expression levels of c-myc, cyclinD1, MMP-7, and annexin-2 were measured by real-time PCR.

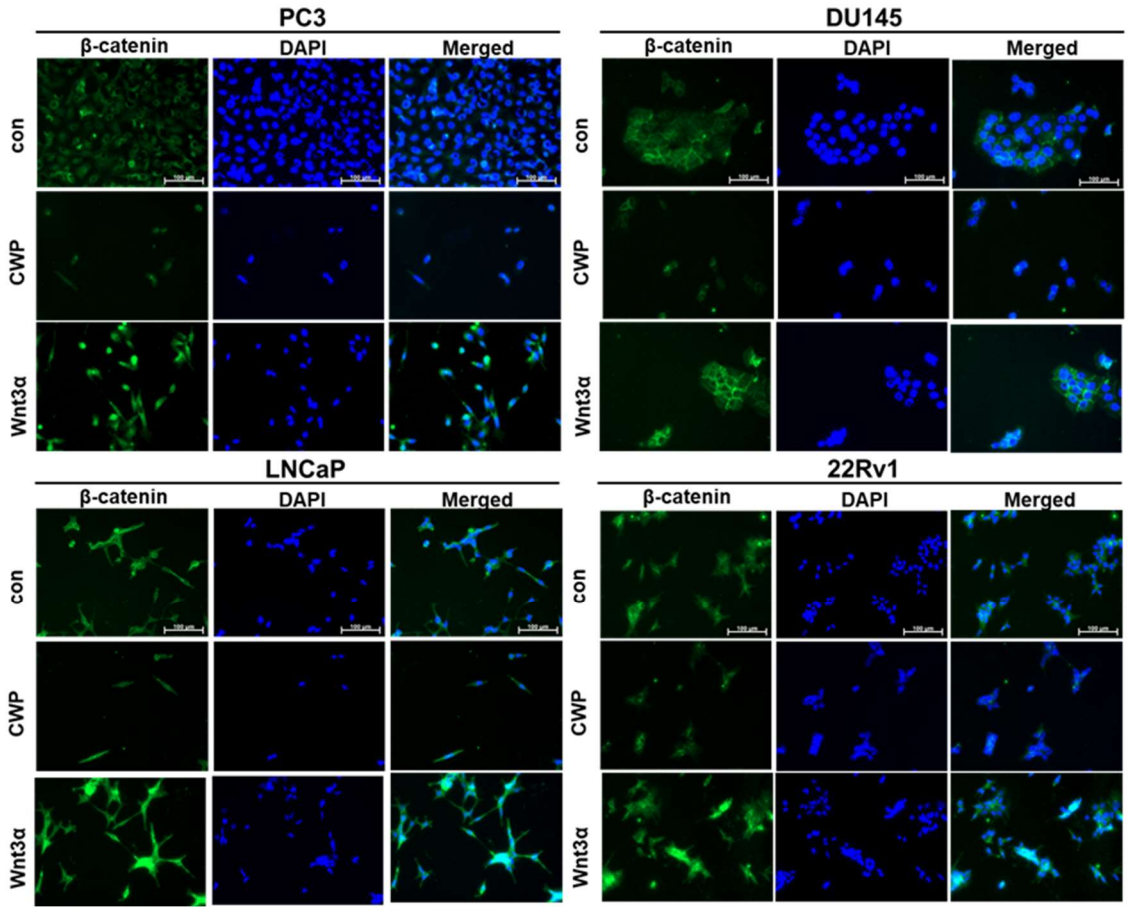

Figure 2. Prostate cancer cells were treated with WNT3A and CWP291 for 24h and stained with β-catenin (green) or DAPI (blue). Images were obtained from a fluorescence microscope.

Downregulation of ARs and splice variants by CWP291

We investigated the impact of CWP291 on AR activity, considering the interaction of β-catenin and ARs in prostate cancer. According to AR status, prostate cancer cells used in these experiments were categorized as follows: AR negative (PC3 and DU145), wild-type AR (LNCaP), AR splice variant positive (22Rv1), and AR overexpressed (VCaP).

After AR-negative (PC3 and DU145) and AR-positive (LNCaP, 22Rv1, and VCaP) prostate cancer cells treated with 0–10 μM CWP291 for 72 h, cell viability was evaluated (Fig. 3A). CWP291 suppressed the growth of prostate cancer cells. In AR-negative cells, the IC_{50} concentrations were higher than those in AR-positive cells (Fig. 3B). To explore whether CWP291 has cytotoxic activity in prostate cancer cells, an LDH-based cytotoxic assay was performed (Fig. 4). Released LDH, a cytotoxicity indicator, was increased at CWP291 concentrations higher than 0.01 μM. Western blotting revealed that CWP291 suppressed the expression of ARs and splice variants

in both LNCaP and 22Rv1 cells (Fig. 3C). Similarly, confocal microscopy and immunofluorescence staining showed that CWP291 markedly suppressed AR expression in both LNCaP and 22Rv1 cells (Fig. 3D).

Previous studies have demonstrated that β-catenin modulates AR transcription via TCF/LEF binding sites within AR promoters (16). To explore whether CWP291 directly inhibits AR transcriptional activity, AR mRNA levels and downstream genes were evaluated in prostate cancer cells (Fig. 3E). LNCaP and 22Rv1 cells were androgen-deprived for 48 h and treated with or without DHT and CWP291. As shown in Fig. 4E, mRNA levels of ARs, prostate-specific antigen (PSA), UBE2C, and TMPRSS2 decreased after treatment, indicating that CWP291 may directly target AR transcriptional activity. Next, we performed an androgen response elements reporter assay. We observed that CWP291 reduced luciferase (androgen response element) activity in prostate cancer cells that were treated with DHT (Fig. 5). The chromatin immunoprecipitation assay showed that β-catenin occupancy of the TCF/LEF-binding

site within the AR promoter was significantly reduced after CWP23221 treatment (Fig. 6), indicating transcriptional regulation of AR by β-catenin.

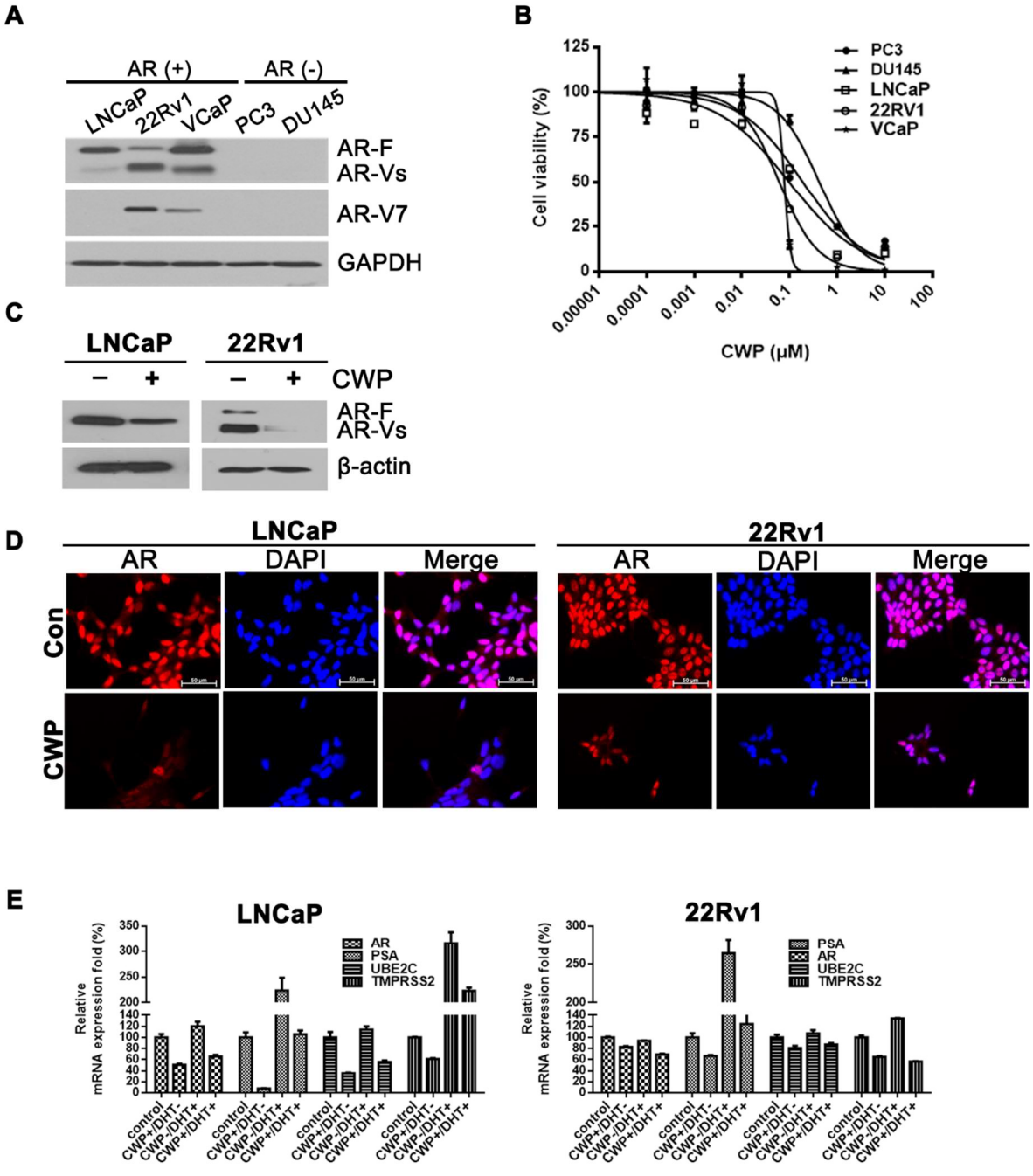

Figure 3. CWP291 downregulates the ARs and splice variants.

(A) AR expression status in prostate cancer cells. Western blotting was conducted

using antibodies for AR, AR-Vs, and AR-V7.

(B) Prostate cancer cells were treated with 0–10 μM CWP291 for 72 h. Cell viability was analyzed with CellTiter Glo® (means ± SD, n=3).

(C) LNCaP and 22Rv1 cells were treated with CWP291 for 72 h. Western blot analysis was conducted using antibodies for AR-F and AR-Vs.

(D) LNCaP and 22Rv1 cells were treated with CWP291 for 24 h and stained with AR (red) or DAPI (blue). Images were obtained via fluorescence microscopy.

(E) LNCaP and 22Rv1 cells were androgen-deprived for 48 h and treated with vehicle or 1 nM DHT with or without CWP291 for 24 h at the IC_{50}. mRNA expression levels of AR, PSA, UBE2C, and TMPRSS2 were measured by real-time PCR.

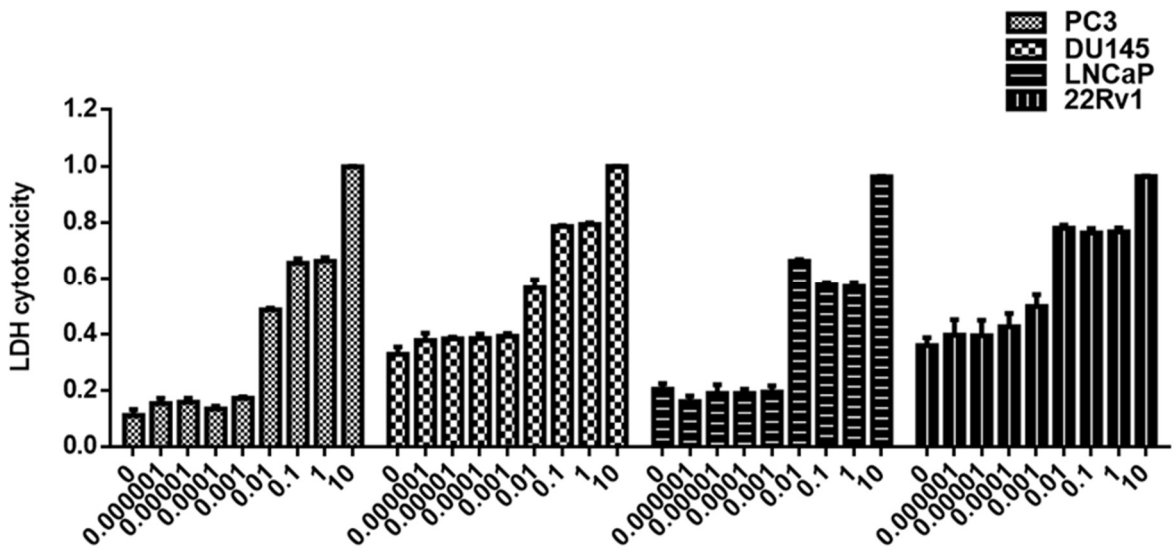

Figure 4. Prostate cancer cells were treated with 0–10 μM CWP291 for 72 h. The LDH cell cytotoxicity was evaluated with the Cytotoxicity Detection Kit.

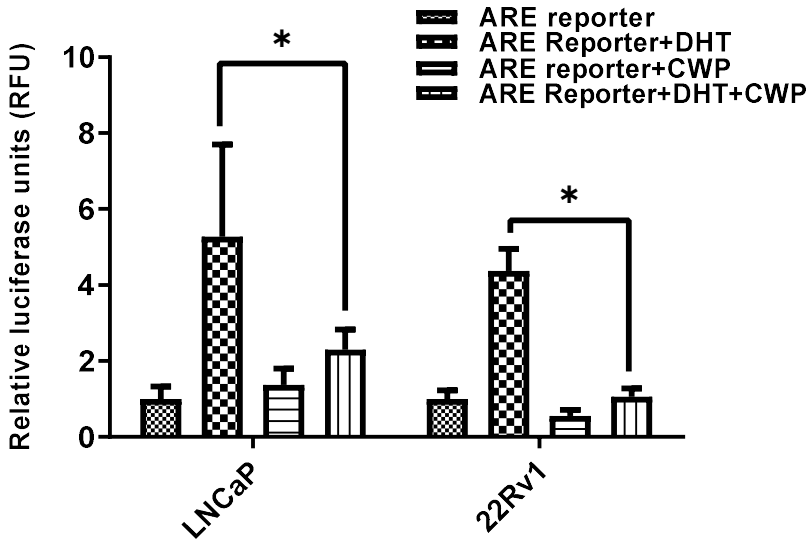

Figure 5. Androgen response elements reporter assay in LNCaP and 22Rv1 cells treated with or without DHT and CWP291 at the IC_{50}.

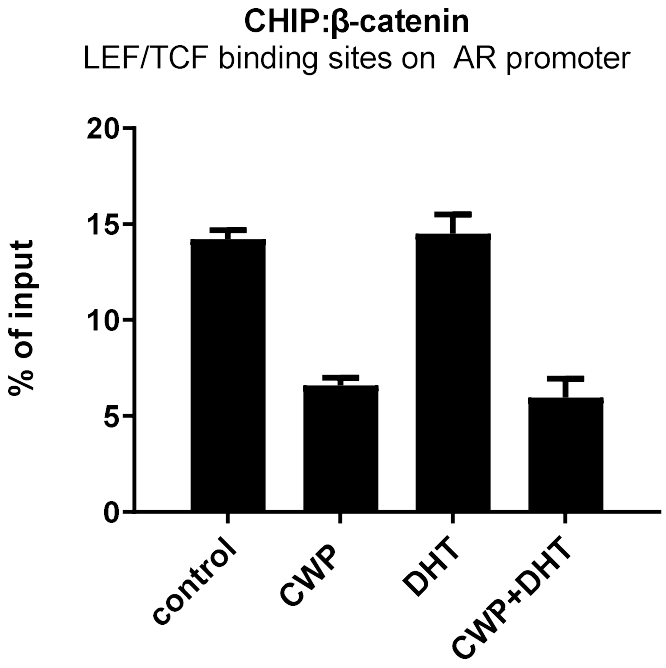

Figure 6. 22Rv1 cells were androgen deprived for 48 h and treated with vehicle or DHT with or without CWP291 for 24 h.

Suppression of the growth of prostate cancer cells by CWP291

We investigated the antitumor activity of CWP291 in prostate cancer cells and compared the effects with those of a conventional chemotherapeutic agent. We treated 22Rv1 and VCaP cells, which are androgen-independent and AR-expressing, with docetaxel or CWP291. In a pattern similar to that associated with docetaxel, CWP291 suppressed the proliferation of both prostate cancer cell types (Fig. 7A). Additionally, CWP291 exerted growth inhibition in docetaxel-resistant DU145 cells as in parental DU145 cells (Fig. 7B). Next, primary prostate cancer cells derived from four CRPC patients were treated with 0–10 μM CWP291 for 72 h (Fig. 7C). Three patients (P1–3) were given docetaxel, and one patient (P4) experienced treatment failure to prechemotherapy enzalutamide. CWP291 had potent antitumor activity against primary prostate cancer cells, independent of previous treatments (Fig. 7C). Interestingly, docetaxel was not effective in primary cells from a patient who was treated with enzalutamide, whereas CWP291 exerted antitumor effects in these cells.

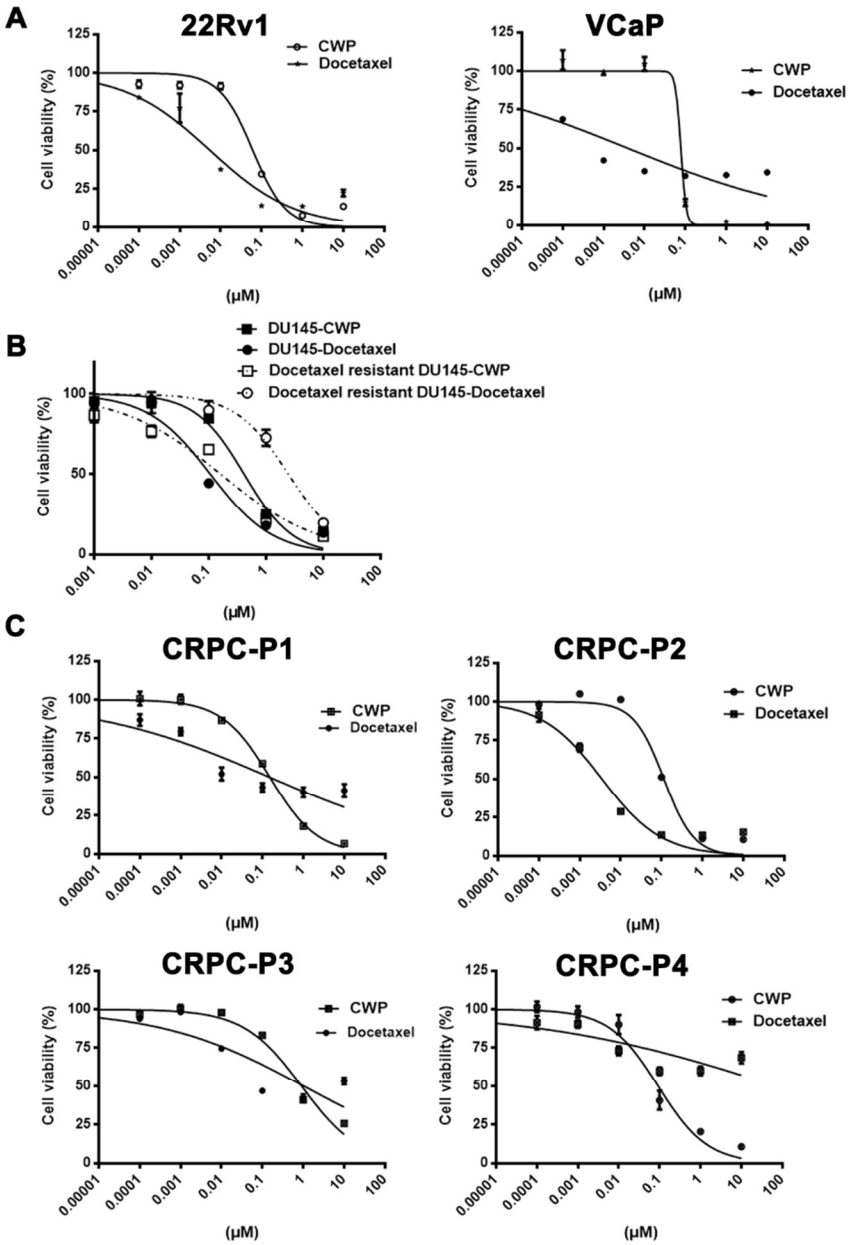

Figure 7. CWP291 suppresses the growth of prostate cancer cells and primary cells derived from patients.

(A) 22Rv1 and VCaP cells were exposed to 0–10 μM CWP291 and 0–10 μM docetaxel for 72 h. Cell viability was analyzed with CellTiter Glo®.

(B) Docetaxel-resistant DU145 and parental DU145 cells were treated with 0–10 μM CWP291 and 0–10 μM docetaxel for 72 h. Cell viability was analyzed with CellTiter Glo®.

(C) Primary castration-resistant prostate cancer cells derived from patients were treated with 0–10 μM CWP291 and 0–10 μM docetaxel for 72 h. Cell viability was analyzed with CellTiter Glo®.

Induction of ER stress by CWP291

We explored whether CWP291 triggers ER stress and subsequent UPR-mediated apoptosis. UPR is activated via three ER stress sensors: inositol-requiring enzyme 1 (IRE1), activating transcription factor 6 (ATF6), and protein kinase RNA-like ER kinase (PERK) (36). Each ER stress sensor uses a unique mechanism to upregulate a subset of UPR target genes (37). IRE1 activation induces degradation of mRNA encoding for ER-located proteins. ATF6 translocates to the Golgi apparatus under ER stress, leading to ER-associated degradation. PERK activation inhibits global protein translation through the phosphorylation of eukaryotic translation initiation factor 2α (eIF2α). Finally, PERK positively controls CHOP, which plays a critical role in UPR-mediated apoptosis (38).

The activity of ER stress markers was evaluated by Western blot and real-time PCR analyses after prostate cancer cells were treated with CWP291 for 24 h at the IC_{50} (Fig. 8). We observed a dose-dependent increase in the phosphorylation of eIF2α, IRE1, and

CHOP protein, along with increased mRNA expression, indicating induction of ER stress by CWP291.

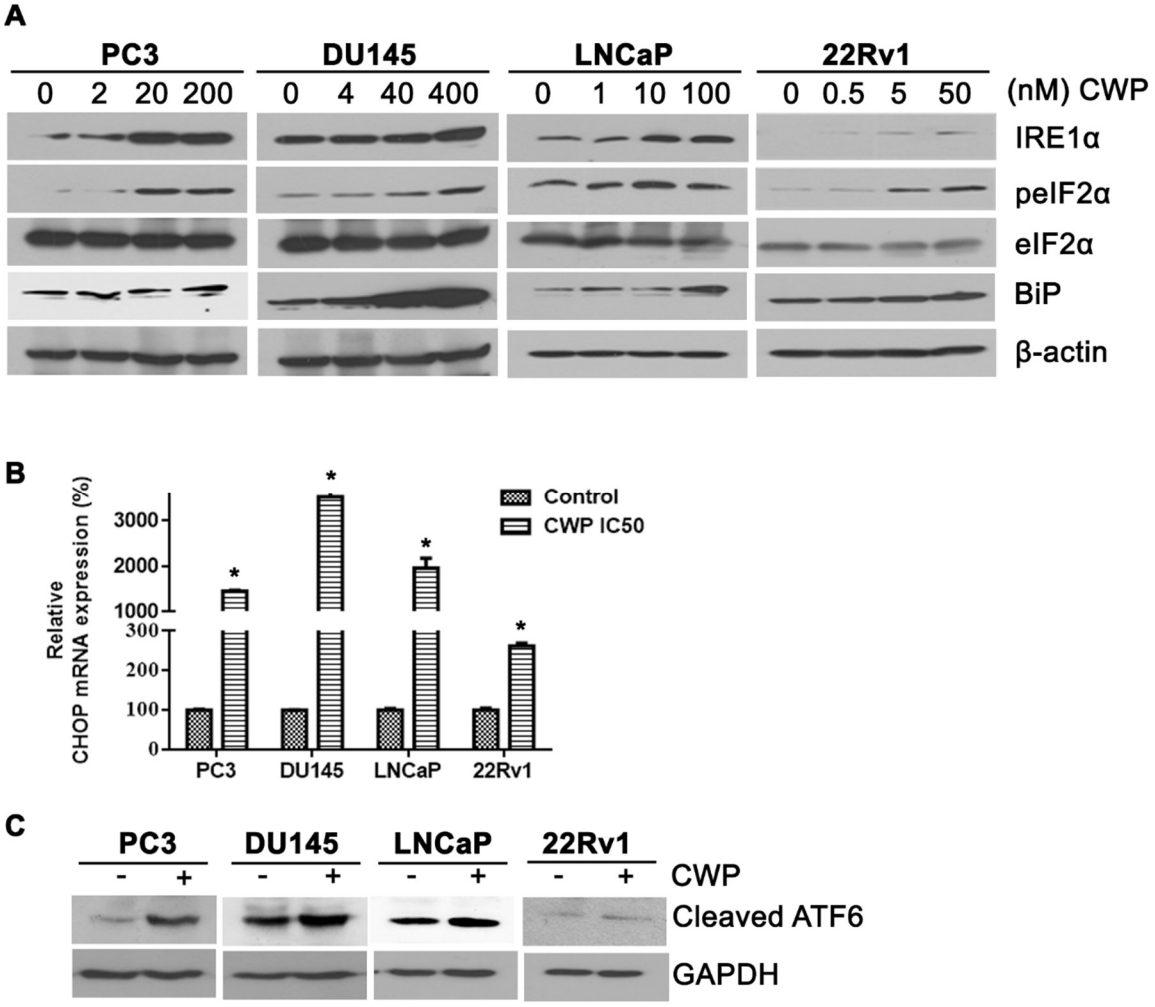

Figure 8. CWP291 triggers endoplasmic reticulum stress and the unfolded protein response in prostate cancer cells.

(A) Prostate cancer cells were treated with CWP291 for 24 h. Western blotting was conducted using antibodies for endoplasmic reticulum stress markers.

(B) Prostate cancer cells were treated with CWP291 for 24 h. CHOP mRNA expression levels were measured by real-time PCR.

(C) Prostate cancer cells were treated with CWP291 for 24 h. Cleaved ATF6 was evaluated by Western blotting.

Induction of apoptosis by CWP291 in prostate cancer cells

Flow cytometry using annexin V and PI was performed to test whether CWP291 induces apoptosis in prostate cancer cell lines (Fig. 9A). Treatment with an IC_{50} dose of CWP291 for 72 h significantly enhanced apoptotic cell death compared with the control in all prostate cancer cells. Additionally, cleaved caspase-3 and PARP-1 levels were markedly increased after CWP291 treatment (Fig. 9B). Overexpression of mRNA levels of Axin-2, a negative modulator of WNT signaling, was observed after CWP291 treatment (Fig. 9C). The cell-permeable pan-caspase inhibitor ZVAD-FMK significantly reduced apoptosis, indicating that cell death by CWP291 occurred through the caspase pathway (Fig. 9D). Together, these results suggest that CWP291 triggers ER stress and the UPR, leading to activation of CHOP and a caspase-3 apoptotic cascade.

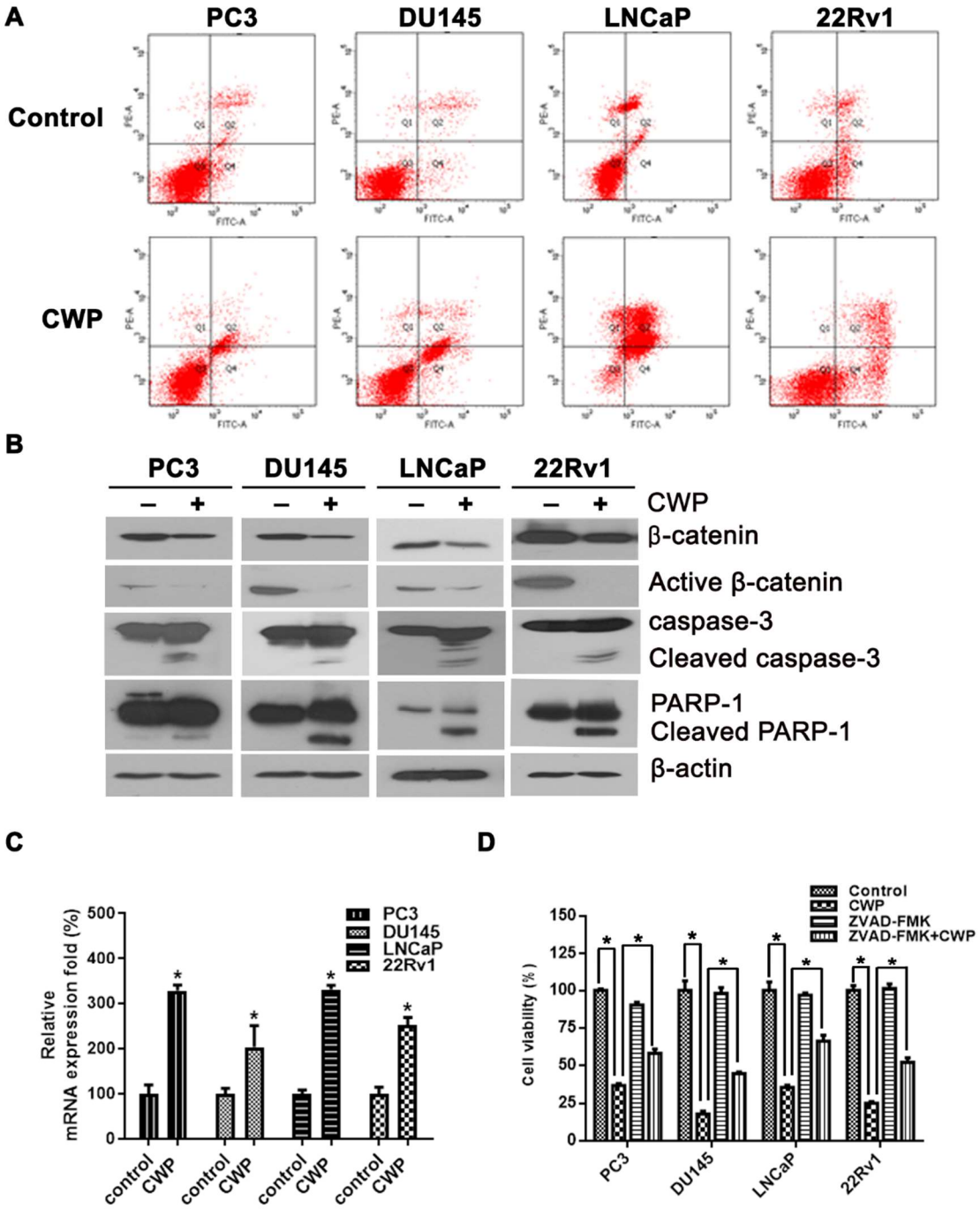

Figure 9. CWP291 mediates cell cycle arrest and apoptosis in prostate cancer cells.

(A) Prostate cancer cells were treated with CWP291 for 72 h. Annexin V/PI-labeled

cells were evaluated with flow cytometry.

(B) Prostate cancer cells were treated with CWP291 for 72 h. β-catenin, caspase, PARP-1 protein changes were evaluated with Western blot analysis.

(C) Prostate cancer cells were treated with CWP291 for 24 h. Axin-2 mRNA expression levels were measured by real-time PCR.

(D) Prostate cancer cells were treated with CWP291 for 96 h with or without 10 μmol/L Z-VAD-FMK. Cell viability was analyzed with CellTiter Glo®.

Prostate cancer xenograft experiments

The in vivo antitumor activity of CWP291 was assessed in the 22Rv1 xenograft mouse model (Fig. 10). The 22Rv1 tumor-bearing mice were treated with CWP291 (50 mg/kg or 100 mg/kg, 27 days). CWP291 suppressed tumor growth compared with the control (Fig. 10A). While body weight did not change significantly after 27 days of CWP291 treatment, tumor growth inhibition rates were 52% (50 mg/kg) and 74% (100 mg/kg) (Fig. 10B). CWP291 markedly decreased tumor weight (50 mg/kg, 245 mg; 100 mg/kg, 160 mg; control, 592 mg) after 27 days compared with the control (Fig. 10C-D). Western blot analysis revealed that CWP291 reduced β-catenin expression and increased cleaved caspase-3 activity compared with the control, suggesting WNT-inhibiting and proapoptotic activity in vivo in a dose- and time-dependent manner (Fig. 10E).

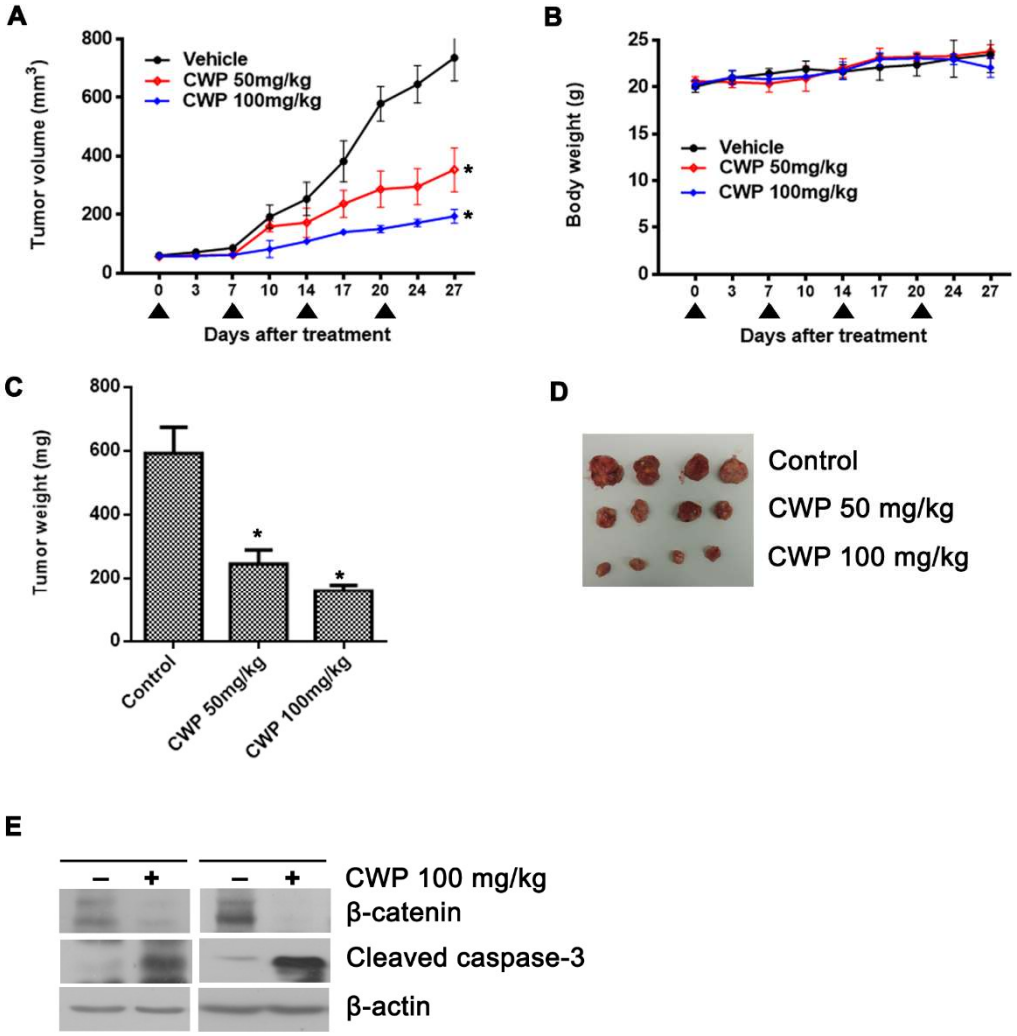

Figure 10. CWP291 suppresses the growth of prostate cancer xenografts.

(A) We treated 22Rv1 tumor-bearing mice with CWP291 (50 mg/kg/day or 100 mg/kg/day, 27 days). Tumor volume changes in the 22Rv1 xenograft mouse model are

presented. Results are shown as means ± SD of six mice.

(B) Body weight of the 22Rv1 tumor-bearing mice is presented. Results are shown as means ± SD.

(C) Tumor weight of the 22Rv1 tumor-bearing mice is presented. Results are shown as means ± SEM.

(D) Representative tumors of the 22Rv1 xenograft mouse model.

(E) Protein levels of β-catenin and cleaved caspase-3 were analyzed by Western blotting. One Western blot was randomly selected from the treatment group and one from the control group.

Sensitivity to AA in 22Rv1 cells and development of AA-resistant prostate cancer cell lines

AA exhibits growth inhibition in 22Rv1 cells (Fig. 11), indicating that 22Rv1 cells are sensitive to AA. We established several stable AA-resistant prostate cancer cell lines by adapting parental 22Rv1 cells to increasing AA concentrations up to 50 μM, and the surviving cells were maintained in 5 μM AA for over 8 weeks. As shown in Fig. 11, 400 nM abiraterone treatment efficiently reduced 22Rv1 cell proliferation, while 22Rv1-AbiR cells in the presence of 1 μM abiraterone exhibited less growth inhibition than parental 22Rv1 cells.

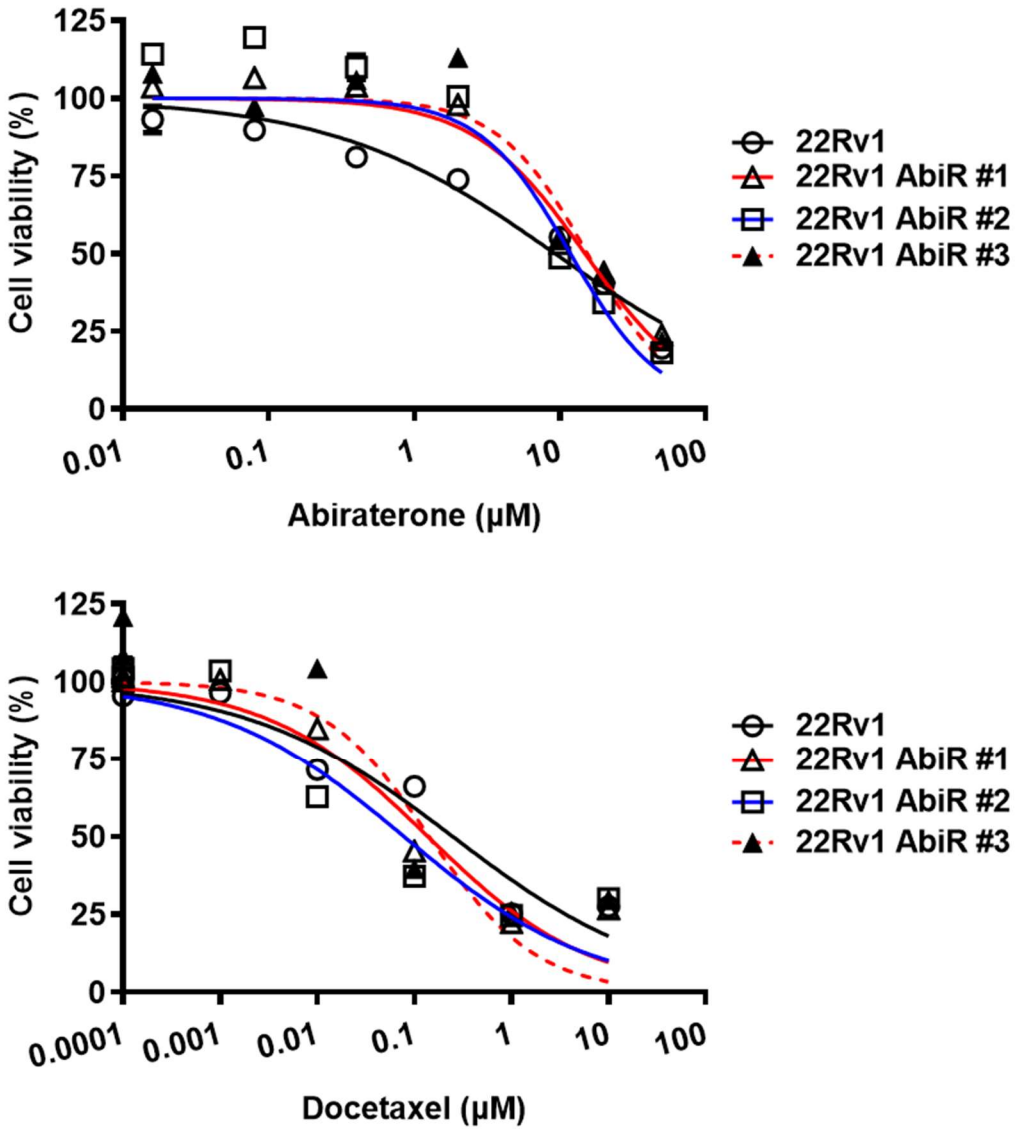

Figure 11. 22Rv1 and 22Rv1-AbiR cells were exposed to 0–100 μM abiraterone acetate and 0–10 μM docetaxel for 72 h. Cell viability was analyzed with CellTiter Glo®.

CWP291 decreases AA-resistant cell proliferation

We investigated whether CWP291 exhibits antitumor activity in AA-resistant prostate cancer cells. Cell viability assays showed that CWP291 treatment decreased cell proliferation in both abiraterone-resistant cell and parental 22Rv1 cells in a concentration-dependent manner (Fig. 12). Next, the inhibition of WNT/β-catenin signaling in 22Rv1-AbiR cells by CWP291 was investigated (Fig. 13). Western blotting revealed that CWP291 significantly suppressed the expression of the β-catenin in AA-resistant prostate cancer cells (Fig. 13A). The 22Rv1-AbiR cells were transfected with a TCF/LEF luciferase reporter plasmid and treated with or without WNT3A (Fig. 13B). CWP291 significantly reduced luciferase activity compared with the control, indicating inhibition of β-catenin transcription in AA-resistant cells. In addition, Western blot and RT-PCR analyses demonstrated downregulation of AR, AR-V7, and AKR1C3 as well as induction of ER stress after CWP291 treatment in AA-

resistant cells (Fig. 13C-F). AKR1C3 has distinct effects on steroidogenesis and its activation confers resistance to AA through increasing intracrine androgen synthesis and enhancing AR signaling (39). Consistent with this, in our results, AKR1C3 was overexpressed in AA-resistant prostate cancer cells (Fig. 13C). The synergistic relationship between AKR1C3 and β-catenin is well documented (40). One previous study showed that the development of AA-resistance is associated with AKR1C3 overexpression and inhibition of AKR1C3 overcomes AA-resistance (39). These results suggest that CWP291 treatment effected antitumor activity in AA-resistant prostate cancer cells through inhibition of β-catenin and AKR1C3, which were upregulated in AA-resistance development.

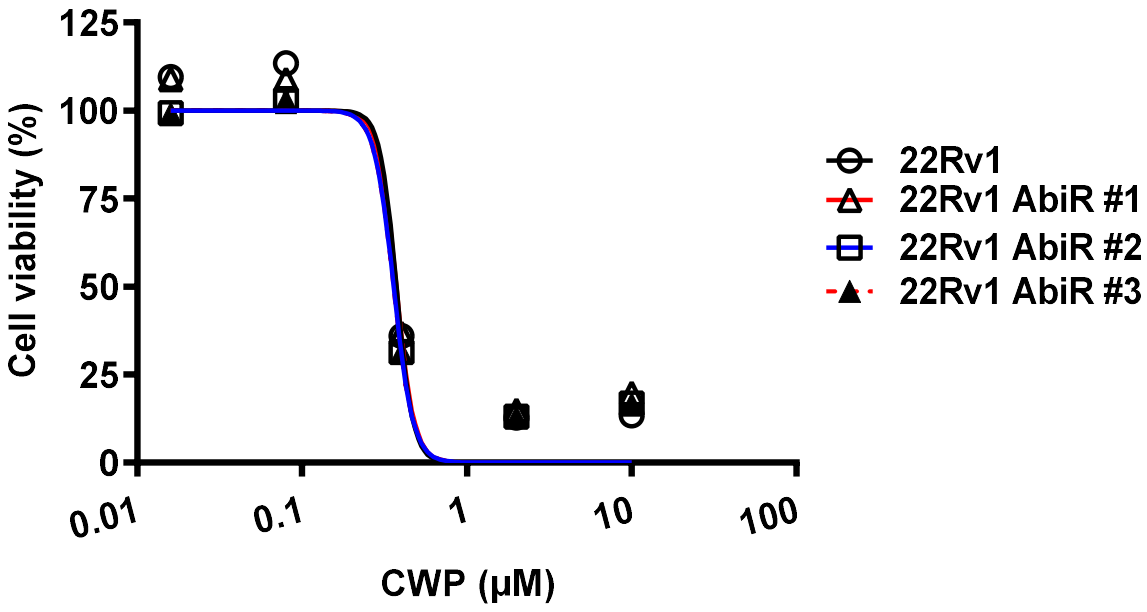

Figure 12. 22Rv1 and 22Rv1-AbiR cells were exposed to 0–10 µM CWP291 for 72 h. Cell viability was analyzed with CellTiter Glo®.

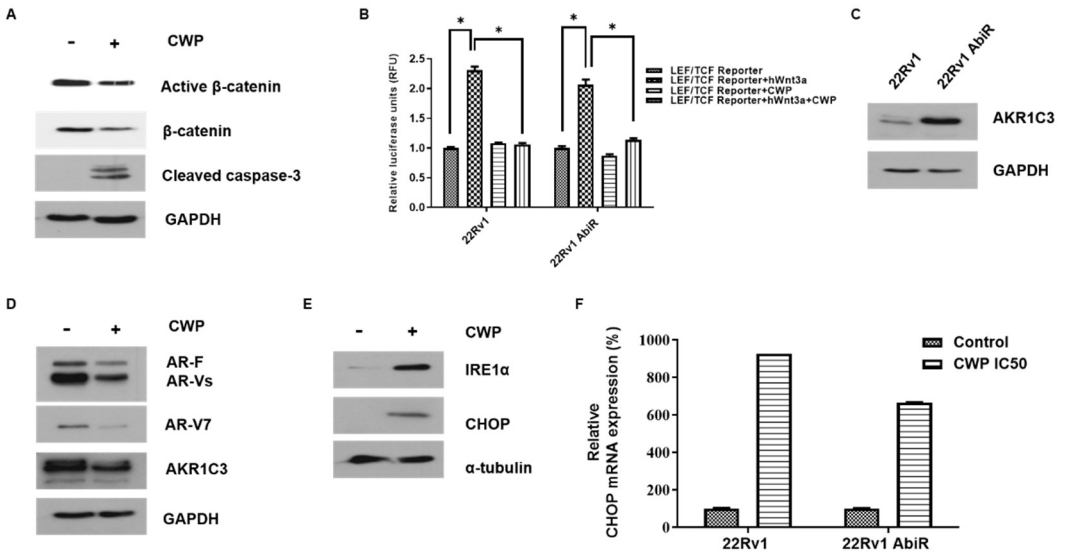

Figure 13. CWP291 regulates WNT, AR, and ER stress signaling in AA-resistant prostate cancer cells.

(A) 22Rv1-AbiR cells were treated with CWP291 for 24 h. Protein levels of β-catenin, survivin, and bcl-2 were evaluated by Western blotting.

(B) Luciferase reporter assay for WNT signaling after treatment with or without WNT3A (100 ng/mL) and CWP291 in 22Rv1-AbiR cells.

(C) Protein levels of AKR1C3 in 22Rv1 and 22Rv-AbiR cells were evaluated by Western blotting.

(D) 22Rv1-AbiR cells were treated with CWP291 for 24 h. Protein levels of AR-F, AR-Vs, AR-V7, and AKR1C3 were evaluated by Western blotting.

(E) 22Rv1-AbiR cells were treated with CWP291 for 24 h. Protein levels of IRE1α and CHOP were evaluated by Western blotting.

(F) 22Rv1-AbiR cells were treated with CWP291 for 24 h. CHOP mRNA expression levels were measured by real-time PCR.

Discussion

This study established that WNT/β-catenin pathway signaling is upregulated in CRPC. Regulation of WNT pathway and ER stress signaling suppresses β-catenin and ARs in prostate cancer cells. Potent antitumor activity was observed in CRPC cells in vitro, ex vivo, and in vivo. Additionally, the WNT signaling pathway is associated with AA treatment, which is the standard of care for CRPC treatment. Our results show that targeting WNT signaling may be a promising novel strategy for CRPC and overcoming AA resistance.

Androgens and ARs play major roles in the development and progression of prostate cancer (9). For patients with advanced prostate cancer, ADT is the most widely used first-line treatment; however, resistance to ADT develops in nearly all patients (10). In CRPC, androgens and ARs still play crucial roles through de novo intratumoral androgen synthesis and circulating adrenal androgens (41). Based on this AR-

dependent mechanism, several second-generation AR-targeted agents, such as AA, enzalutamide, apalutamide, and darolutamide (42), were introduced and approved for standard prostate cancer treatment. Despite these AR-signaling inhibitors prolonging survival outcomes, approximately a quarter of patients do not respond initially, and drug resistance occurs in nearly all patients who respond (43).

In this study, we observed that WNT signaling pathway regulation is effective in CRPC cells. The WNT signaling pathway includes both canonical and noncanonical pathways (44). The canonical pathway is activated upon binding of WNT ligands to Fzd receptors. Noncanonical WNT signals are categorized into two pathways: the WNT/planar cell polarity (PCP) pathway and the WNT-cGMP/Ca^{2+} pathway (45). Mutation-induced WNT pathway activation is a common driving event in human cancer (46). WNT signaling activation provides sustained self-renewing growth properties to cancer cells and contributes to treatment resistance. Several recent studies have demonstrated the close association between the WNT signaling pathway and

prostate cancer development and progression (44, 45, 47, 48). Additionally, some studies have reported that WNT signaling is associated with resistance to treatment in CRPC (44, 47). It is well known that malignancies harbor a subpopulation of cancer stem cells that plays roles in oncogenesis and tumor progression (49-51). In prostate cancer, stem cells fuel the development of castration resistance, independent of androgen (52). Given that WNT plays a pivotal role in stem cell control, the WNT pathway may be a promising anticancer target (14, 53). However, the role and modulation of WNT signaling in CRPC remain largely unknown.

This study revealed that WNT/β-catenin inhibition suppresses the growth of CRPC cells and primary prostate cancer cells. Our data showed that WNT signaling inhibition downregulates the activity of ARs and splice variants in CRPC cells. Targeting the WNT pathway may be particularly effective against CRPC given the crosstalk of β-catenin and ARs (16-22). β-catenin and ARs interact synergistically to enhance hormone-independent growth in androgen-deprived environments (54). Consistent

with this, in our results, the antitumor activity of WNT signaling inhibition was more pronounced in AR-positive prostate cancer cells, such as LNCaP, 22Rv1, and VCaP, than in AR-negative cells (PC3 and DU145). Our data indicate that WNT signaling inhibition could be more effective for AR-expressing CRPC compared with AR-negative disease via the disruption of AR and β-catenin interactions.

There is evidence that WNT signaling activation induces resistance to chemotherapeutic agents in solid malignancies (55-57), highlighting the role of WNT signaling regulation in the treatment of chemoresistant disease (58, 59). Our finding that CWP291 exerted potent antitumor effects in docetaxel-resistant cells supports that hypothesis.

Additionally, our results suggest that the WNT signaling pathway is associated with AA resistance. This study showed that the small molecule CWP291 suppresses the proliferation of AA-resistant prostate cancer cells by suppressing WNT/β-catenin signaling. AA is an orally administered selective inhibitor of cytochrome P450

17alpha-hydroxylase/17, 20 lyase (CYP17A1), which plays a key role in sex steroid synthesis (10). AA suppresses AR signaling and intratumoral androgen production. AA has become a standard-of-care treatment option for patients with advanced prostate cancer (60). AA has been reported to prolong overall survival by an average of 5 months and time to PSA progression by 1.9 months among patients with metastatic CRPC (61). However, secondary resistance to AA eventually develops in nearly all patients, while a quarter of patients do not respond initially.

Several studies have investigated potential mechanisms of AA resistance (41, 47, 60, 62, 63). Increased expression of full-length ARs, AR variants, and CYP17A1 were observed in CRPC xenografts treated with AA (62), suggesting that AR splice variants and upregulation of CYP17A1 might be associated with AA resistance (63). Some studies have examined the relationship between WNT signaling and resistance to AR signaling inhibitors in CRPC (41, 44, 47, 64). Chen et al. reported that noncanonical WNT signaling was activated in enzalutamide-resistant prostate cancer cells and that

the activation of noncanonical WNT signaling was correlated with AR expression and disease progression (44). Pan et al. reported that AA resistance is associated with enhanced CBP/p300 activity, which is associated with transcription regulation in the WNT pathway, leading to global gene expression alterations (64). Velho et al. reported that patients with WNT pathway–activating mutations have worse PSA progression–free and overall survival outcomes in association with first-line abiraterone/enzalutamide treatment than WNT wild-type patients (47).

We established AA-resistant prostate cancer cells from a parental 22Rv1 cell line. We observed that WNT/β-catenin inhibition downregulated full-length ARs, AR-V7, and AKR1C3. Additionally, CWP291 blocks the growth of AA-resistant prostate cancer cells through suppression of WNT/β-catenin signaling and ER stress induction. Mechanistically, CWP291 inhibits AKR1C3 activation, which drives resistance to AA through increasing intracrine androgen synthesis and enhancing AR signaling (39).

However, these AA-resistant cell line experiments had several limitations. First, we

only investigated WNT pathway modulation in AR-positive 22Rv1 cells in this study. As mentioned above, WNT pathway modulation may be more effective in AR-expressing prostate cancer because of the crosstalk between β-catenin and ARs. Second, we did not examine prostate cancer cells resistant to other AR signaling inhibitors, such as enzalutamide, darolutamide, or apalutamide. The potential relationship between WNT signaling and resistance to AA may not be applicable to other AR signaling inhibitors due to varying drug mechanisms. Third, we did not investigate antitumor activity in AA-resistant prostate cancer cells ex vivo and in vivo.

Several pharmacological agents that modulate WNT signaling have been developed and tested in clinical trials (59). Though research efforts regarding WNT signaling in malignant diseases continue, no WNT signaling modulator has been approved to date. CWP291, which was used in this study, has been tested in clinical trials investigating treatments for hematologic malignancies (34, 65, 66) and has shown a favorable safety profile. A major concern with the use of WNT signaling regulation is off-target effects

since the WNT pathway plays a critical role in normal stem cell control (67).

CWP291 does not only inhibit WNT/β-catenin activity; it also induces ER stress. The ER has recently emerged as a promising anticancer target. Several cytotoxic agents that target the ER exhibit selectivity for cancer cells over noncancer cells, and ER stress induction often leads to immunogenic cell death (68). We observed that CWP291 triggers ER stress in prostate cancer cells. Upon the induction of ER stress, sequential occurrence of stress sensor PERK activation, eIF2α phosphorylation, and proapoptotic CHOP upregulation ensues, leading to downstream caspase-3–dependent apoptosis. Our data show that ER stress induction can exert antitumor activity in CRPC. Interestingly, ER stress is associated with WNT/β-catenin signaling. Previous studies have demonstrated that caspase-3-dependent apoptosis by ER stress induction can degrade β-catenin and abrogate processing and secretion of WNT protein (69-71).

Conclusions

In summary, this study demonstrated that the small molecule CWP291, a WNT/β-catenin inhibitor and ER stress inducer, suppresses the growth of CRPC cells in vitro, ex vivo, and in vivo. WNT inhibition suppresses the activity of ARs and splice variants in CRPC. WNT signaling inhibition was also associated with potent antitumor activity against AA-resistant CRPC cells. Our results provide preclinical evidence supporting a therapeutic strategy for CRPC involving WNT/β-catenin signaling and ER stress pathway modulation.

References

1. Bray F, Ferlay J, Soerjomataram I, Siegel RL, Torre LA, Jemal A. Global cancer statistics 2018: GLOBOCAN estimates of incidence and mortality worldwide for 36 cancers in 185 countries. CA: a cancer journal for clinicians. 2018;68(6):394-424.

2. Grossman DC, Curry SJ, Owens DK, Bibbins-Domingo K, Caughey AB, Davidson KW, et al. Screening for prostate cancer: US Preventive Services Task Force recommendation statement. Jama. 2018;319(18):1901-13.

3. Murthy V, Mallick I, Gavarraju A, Sinha S, Krishnatry R, Telkhade T, et al. Study protocol of a randomised controlled trial of prostate radiotherapy in high-risk and node-positive disease comparing moderate and extreme hypofractionation (PRIME TRIAL). BMJ open. 2020;10(2):e034623.

4. Mayer M, Klotz L, Venkateswaran V. Metformin and prostate cancer stem cells: a novel therapeutic target. Prostate cancer and prostatic diseases. 2015;18(4):303-9.

5. De Bono JS, Logothetis CJ, Molina A, Fizazi K, North S, Chu L, et al. Abiraterone and increased survival in metastatic prostate cancer. New England Journal of Medicine. 2011;364(21):1995-2005.

6. Scher HI, Fizazi K, Saad F, Taplin M-E, Sternberg CN, Miller K, et al. Increased survival with enzalutamide in prostate cancer after chemotherapy. New England Journal of Medicine. 2012;367(13):1187-97.

7. Lowrance WT, Roth BJ, Kirkby E, Murad MH, Cookson MS. Castration-resistant prostate cancer: AUA guideline amendment 2015. The Journal of urology. 2016;195(5):1444-52.

8. de Porras VR, Font A, Aytes A. Chemotherapy in metastatic castration-resistant prostate cancer: Current scenario and future perspectives. Cancer Letters. 2021.

9. Murillo-Garzón V, Kypta R. WNT signalling in prostate cancer. Nature Reviews Urology. 2017;14(11):683.

10. Antonarakis ES, Lu C, Wang H, Luber B, Nakazawa M, Roeser JC, et al. AR-V7 and resistance to enzalutamide and abiraterone in prostate cancer. New England Journal of Medicine. 2014;371(11):1028-38.

11. Logan CY, Nusse R. The Wnt signaling pathway in development and disease. Annu Rev Cell Dev Biol. 2004;20:781-810.

12. Kim N-G, Xu C, Gumbiner BM. Identification of targets of the Wnt pathway destruction complex in addition to β-catenin. Proceedings of the National Academy of Sciences. 2009;106(13):5165-70.

13. Nguyen VHL, Hough R, Bernaudo S, Peng C. Wnt/β-catenin signalling in ovarian cancer: Insights into its hyperactivation and function in tumorigenesis. Journal of ovarian research. 2019;12(1):1-17.

14. Clevers H, Nusse R. Wnt/β-catenin signaling and disease. Cell. 2012;149(6):1192-205.

15. Grasso CS, Wu Y-M, Robinson DR, Cao X, Dhanasekaran SM, Khan AP, et al. The mutational landscape of lethal castration-resistant prostate cancer. Nature. 2012;487(7406):239.

16. Lee E, Madar A, David G, Garabedian MJ, DasGupta R, Logan SK. Inhibition of androgen receptor and β-catenin activity in prostate cancer. Proceedings of the National Academy of Sciences. 2013;110(39):15710-5.

17. Schneider JA, Logan SK. Revisiting the role of Wnt/β-catenin signaling in prostate cancer. Molecular and cellular endocrinology. 2017.

18. Schweizer L, Rizzo CA, Spires TE, Platero JS, Wu Q, Lin T-A, et al. The androgen receptor can signal through Wnt/β-Catenin in prostate cancer cells as an adaptation mechanism to castration levels of androgens. BMC cell biology. 2008;9(1):4.

19. Song L-N, Herrell R, Byers S, Shah S, Wilson EM, Gelmann EP. β-Catenin binds to the activation function 2 region of the androgen receptor and modulates the effects of the N-terminal domain and TIF2 on ligand-dependent transcription. Molecular and cellular

biology. 2003;23(5):1674-87.

20. Wan X, Liu J, Lu J-F, Tzelepi V, Yang J, Starbuck MW, et al. Activation of β-Catenin Signaling in Androgen Receptor–Negative Prostate Cancer Cells. Clinical cancer research. 2012;18(3):726-36.

21. Wang G, Wang J, Sadar MD. Crosstalk between the androgen receptor and β-catenin in castrate-resistant prostate cancer. Cancer research. 2008;68(23):9918-27.

22. Yang F, Li X, Sharma M, Sasaki CY, Longo DL, Lim B, et al. Linking β-catenin to androgen-signaling pathway. Journal of Biological Chemistry. 2002;277(13):11336-44.

23. Ahmad I, Sansom OJ. Role of Wnt Signalling in Advanced Prostate Cancer. The Journal of pathology. 2018.

24. Chevet E, Hetz C, Samali A. Endoplasmic reticulum stress–activated cell reprogramming in oncogenesis. Cancer discovery. 2015;5(6):586-97.

25. Özcan U, Cao Q, Yilmaz E, Lee A-H, Iwakoshi NN, Özdelen E, et al. Endoplasmic reticulum stress links obesity, insulin action, and type 2 diabetes. Science. 2004;306(5695):457-61.

26. Luo B, Lee AS. The critical roles of endoplasmic reticulum chaperones and unfolded protein response in tumorigenesis and anticancer therapies. Oncogene. 2013;32(7):805.

27. Maurel M, McGrath EP, Mnich K, Healy S, Chevet E, Samali A, editors. Controlling the unfolded protein response-mediated life and death decisions in cancer. Seminars in cancer biology; 2015: Elsevier.

28. Forsythe N, Refaat A, Javadi A, Khawaja H, Weir J-A, Emam H, et al. The unfolded protein response: a novel therapeutic target for poor prognostic BRAF mutant colorectal cancer. Molecular cancer therapeutics. 2018;17(6):1280-90.

29. Fribley A, Zeng Q, Wang C-Y. Proteasome inhibitor PS-341 induces apoptosis through induction of endoplasmic reticulum stress-reactive oxygen species in head and neck squamous cell carcinoma cells. Molecular and cellular biology. 2004;24(22):9695-704.

30. Lamothe B, Wierda W, Keating MJ, Gandhi V. Carfilzomib triggers cell death in

chronic lymphocytic leukemia by inducing proapoptotic and endoplasmic reticulum stress responses. Clinical cancer research. 2016:clincanres. 2522.015.

31. Vandewynckel Y-P, Laukens D, Devisscher L, Bogaerts E, Paridaens A, Van den Bussche A, et al. Placental growth factor inhibition modulates the interplay between hypoxia and unfolded protein response in hepatocellular carcinoma. BMC cancer. 2016;16(1):9.

32. Vincenz L, Jäger R, O'Dwyer M, Samali A. Endoplasmic reticulum stress and the unfolded protein response: targeting the Achilles heel of multiple myeloma. Molecular cancer therapeutics. 2013;12(6):831-43.

33. Pak S, Park S, Kim Y, Park J-H, Park C-H, Lee K-J, et al. The small molecule WNT/β-catenin inhibitor CWP232291 blocks the growth of castration-resistant prostate cancer by activating the endoplasmic reticulum stress pathway. Journal of Experimental & Clinical Cancer Research. 2019;38(1):1-13.

34. Cortes JE, Faderl S, Pagel J, Jung CW, Yoon S-S, Koh Y, et al. Phase 1 study of CWP232291 in relapsed/refractory acute myeloid leukemia (AML) and myelodysplastic syndrome (MDS). American Society of Clinical Oncology; 2015.

35. Bauman TM, Vezina CM, Ricke EA, Halberg RB, Huang W, Peterson RE, et al. Expression and colocalization of β-catenin and lymphoid enhancing factor-1 in prostate cancer progression. Human pathology. 2016;51:124-33.

36. Schröder M, Kaufman RJ. ER stress and the unfolded protein response. Mutation Research/Fundamental and Molecular Mechanisms of Mutagenesis. 2005;569(1):29-63.

37. Hetz C. The unfolded protein response: controlling cell fate decisions under ER stress and beyond. Nature reviews Molecular cell biology. 2012;13(2):89-102.

38. Tabas I, Ron D. Integrating the mechanisms of apoptosis induced by endoplasmic reticulum stress. Nature cell biology. 2011;13(3):184.

39. Liu C, Armstrong CM, Lou W, Lombard A, Evans CP, Gao AC. Inhibition of AKR1C3 activation overcomes resistance to abiraterone in advanced prostate cancer. Molecular cancer therapeutics. 2017;16(1):35-44.

40. Xiong W, Huang X, Hu W. AKR1C3 and β-catenin expression in non-small cell lung cancer and relationship with radiation resistance. Journal of BU ON: Official Journal of the Balkan Union of Oncology. 2021;26(3):802-11.

41. Mostaghel EA, Marck BT, Kolokythas O, Chew F, Evan YY, Schweizer MT, et al. Circulating and Intratumoral Adrenal Androgens Correlate with Response to Abiraterone in Men with Castration-Resistant Prostate Cancer. Clinical Cancer Research. 2021.

42. Mori K, Mostafaei H, Pradere B, Motlagh RS, Quhal F, Laukhtina E, et al. Apalutamide, enzalutamide, and darolutamide for non-metastatic castration-resistant prostate cancer: a systematic review and network meta-analysis. International journal of clinical oncology. 2020:1-9.

43. Saranyutanon S, Srivastava SK, Pai S, Singh S, Singh AP. Therapies targeted to androgen receptor signaling axis in prostate cancer: Progress, challenges, and hope. Cancers. 2020;12(1):51.

44. Chen X, Liu J, Cheng L, Li C, Zhang Z, Bai Y, et al. Inhibition of noncanonical Wnt pathway overcomes enzalutamide resistance in castration-resistant prostate cancer. The Prostate. 2020;80(3):256-66.

45. Chen Y, Chen Z, Tang Y, Xiao Q. The involvement of noncanonical Wnt signaling in cancers. Biomedicine & Pharmacotherapy. 2021;133:110946.

46. Bugter JM, Fenderico N, Maurice MM. Mutations and mechanisms of WNT pathway tumour suppressors in cancer. Nature Reviews Cancer. 2021;21(1):5-21.

47. Velho PI, Fu W, Wang H, Mirkheshti N, Qazi F, Lima FA, et al. Wnt-pathway activating mutations are associated with resistance to first-line abiraterone and enzalutamide in castration-resistant prostate cancer. European urology. 2020;77(1):14-21.

48. Wang Y, Singhal U, Qiao Y, Kasputis T, Chung J-S, Zhao H, et al. Wnt signaling drives prostate cancer bone metastatic tropism and invasion. Translational oncology. 2020;13(4):100747.

49. Jordan CT, Guzman ML, Noble M. Cancer stem cells. New England Journal of

Medicine. 2006;355(12):1253-61.

50. Li Y, Kong D, Ahmad A, Bao B, Sarkar FH. Targeting cancer stem cells for overcoming drug resistance and cancer progression. Cancer Stem Cells. 2014:461-71.

51. Sampieri K, Fodde R, editors. Cancer stem cells and metastasis. Seminars in cancer biology; 2012: Elsevier.

52. Lawson DA, Witte ON. Stem cells in prostate cancer initiation and progression. J Clin Invest. 2007;117(8):2044-50.

53. Anastas JN, Moon RT. WNT signalling pathways as therapeutic targets in cancer. Nature Reviews Cancer. 2013;13(1):11.

54. Yokoyama NN, Shao S, Hoang BH, Mercola D, Zi X. Wnt signaling in castration-resistant prostate cancer: implications for therapy. American journal of clinical and experimental urology. 2014;2(1):27.

55. Flahaut M, Meier R, Coulon A, Nardou K, Niggli F, Martinet D, et al. The Wnt receptor FZD1 mediates chemoresistance in neuroblastoma through activation of the Wnt/β-catenin pathway. Oncogene. 2009;28(23):2245.

56. Li J, Yang S, Su N, Wang Y, Yu J, Qiu H, et al. Overexpression of long non-coding RNA HOTAIR leads to chemoresistance by activating the Wnt/β-catenin pathway in human ovarian cancer. Tumor Biology. 2016;37(2):2057-65.

57. Noda T, Nagano H, Takemasa I, Yoshioka S, Murakami M, Wada H, et al. Activation of Wnt/β-catenin signalling pathway induces chemoresistance to interferon-α/5-fluorouracil combination therapy for hepatocellular carcinoma. British journal of cancer. 2009;100(10):1647.

58. Mohammed MK, Shao C, Wang J, Wei Q, Wang X, Collier Z, et al. Wnt/β-catenin signaling plays an ever-expanding role in stem cell self-renewal, tumorigenesis and cancer chemoresistance. Genes & diseases. 2016;3(1):11-40.

59. Tabatabai R, Linhares Y, Bolos D, Mita M, Mita A. Targeting the Wnt pathway in cancer: a review of novel therapeutics. Targeted oncology. 2017;12(5):623-41.

60. Shpilsky J, Stevens J, Bubley G. An up-to-date evaluation of abiraterone for the treatment of prostate cancer. Expert Opinion on Pharmacotherapy. 2021:1-8.

61. Fizazi K, Scher HI, Molina A, Logothetis CJ, Chi KN, Jones RJ, et al. Abiraterone acetate for treatment of metastatic castration-resistant prostate cancer: final overall survival analysis of the COU-AA-301 randomised, double-blind, placebo-controlled phase 3 study. The lancet oncology. 2012;13(10):983-92.

62. Mostaghel EA, Marck BT, Plymate SR, Vessella RL, Balk S, Matsumoto AM, et al. Resistance to CYP17A1 inhibition with abiraterone in castration-resistant prostate cancer: induction of steroidogenesis and androgen receptor splice variants. Clinical cancer research. 2011;17(18):5913-25.

63. Giacinti S, Bassanelli M, Aschelter AM, Milano A, Roberto M, Marchetti P. Resistance to abiraterone in castration-resistant prostate cancer: a review of the literature. Anticancer research. 2014;34(11):6265-9.

64. Pan W, Zhang Z, Kimball H, Qu F, Berlind K, Stopsack KH, et al. Abiraterone acetate induces CREB1 phosphorylation and enhances the function of the CBP-p300 complex, leading to resistance in prostate cancer cells. Clinical Cancer Research. 2021;27(7):2087-99.

65. Manasanch EE, Yoon S-S, Min C-K, Kim JS, Shain KH, Hauptschein R, et al. Interim Results from the Phase 1a/1b Dose-Finding Study of CWP232291 (CWP291) in Relapsed or Refractory Myeloma (RRMM) Alone or in Combination with Lenalidomide and Dexamethasone. Am Soc Hematology; 2017.

66. Yoon S-S, Min C-K, Kim JS, Manasanch EE, Hauptschein R, Choi J, et al. Ongoing phase 1a/1b dose-finding study of CWP232291 (CWP291) in relapsed or refractory multiple myeloma (MM). Am Soc Hematology; 2016.

67. Takahashi-Yanaga F, Kahn M. Targeting Wnt signaling: can we safely eradicate cancer stem cells? Clinical cancer research. 2010;16(12):3153-62.

68. King AP, Wilson JJ. Endoplasmic reticulum stress: an arising target for metal-based anticancer agents. Chemical Society Reviews. 2020;49(22):8113-36.

69. Maier TJ, Janssen A, Schmidt R, Geisslinger G, Grösch S. Targeting the beta-catenin/APC pathway: a novel mechanism to explain the cyclooxygenase-2-independent anticarcinogenic effects of celecoxib in human colon carcinoma cells. The FASEB journal. 2005;19(10):1353-5.

70. Steinhusen U, Badock V, Bauer A, Behrens J, Wittman-Liebold B, Dörken B, et al. Apoptosis-induced cleavage of β-catenin by caspase-3 results in proteolytic fragments with reduced transactivation potential. Journal of Biological Chemistry. 2000;275(21):16345-53.

71. Verras M, Papandreou I, Lim AL, Denko NC. Tumor hypoxia blocks Wnt processing and secretion through the induction of endoplasmic reticulum stress. Molecular and cellular biology. 2008;28(23):7212-24.

국문요약

거세 저항성 전립선암의 생존율을 향상시키는 치료가 몇 가지 있음에도 불구하고, 거세 저항성 전립선암 환자의 생존 기간 중간 값은 2년 미만에 불과하며, 대부분의 치료는 후천적 내성의 획득으로 진행된다. 많은 연구 결과에 따르면, WNT 신호와 소포체 스트레스는 암의 발생과 진행 과정에서 중요한 역할을 한다. 본 연구에서는 CWP232291 저분자 약물을 이용하여 β-catenin 억제 및 소포체 스트레스 유도가 거세 저항성 전립선암에서 항암 효과가 있는지 알아보고자 하였다.

본 연구에서는 인간 전립선암 세포주와 환자에게서 유래된 일차 세포에서 CWP232291의 효과를 평가하였다. 세포 자멸, WNT/β-catenin 신호 전달 및 소포체 스트레스 반응을 평가하기 위해 Western blotting, 역전사 및 정량적 중합효소 연쇄 반응, 면역형광 염색, 공초점 현미경, 유세포분석, 세포 독성 분석, 이중 발광 효소 분석, Annexin V 및 propidium iodide 분석, 염색질 면역 침전 분석을 사용하였다. 이에 더해, 항암 효과를 평가하기 위하여 22Rv1 이종 이식 마우스 모델을 사용하였다.

CWP232291은 전립선암 세포에서 β-카테닌 활성과 전사를 억제하였으며, androgen 수용체 및 스플라이스 변이체를 하향 조절하였다. 또한, CWP232291은 소포체 스트레스를 유발하여 세포 자멸을 유도하는 C/EBP-homologous 단백질을 상향 조절하고, caspase-3에 의한 세포 사멸 cascade를 활성화하였다. CWP232291은 거세 저항성 전립선암 세포주 및 일차 세포의 성장을 억제하였고, 22Rv1 이종 이식 마우스 모델에서 생체 내 항암 효과 활성을 보였다.

결과를 요약하면, CWP232291은 시험관 내, 생체 외 및 생체 내에서 거세 저항성 전립선암 세포의 성장을 억제하였으며, 이는 WNT/β-catenin 및 소포체 스트레스 조절이 거세 저항성 전립선암의 치료 전략 중 하나가 될 수 있다는 점을 보여준다.